analytical chemistry

Subscriber access provided by NEW YORK UNIV

Article

Protein Binding Bends the Gold Nanoparticle Capped DNA Sequence: Towards Novel Energy-transfer based Photoelectrochemical Protein Detection

Zheng-Yuan Ma, Yi-Fan Ruan, Fei Xu, Wei-Wei Zhao, Jing-Juan Xu, and Hong-Yuan Chen

Anal. Chem., **Just Accepted Manuscript** • DOI: 10.1021/acs.analchem.6b00012 • Publication Date (Web): 11 Mar 2016

Downloaded from http://pubs.acs.org on March 12, 2016

Just Accepted

"Just Accepted" manuscripts have been peer-reviewed and accepted for publication. They are posted online prior to technical editing, formatting for publication and author proofing. The American Chemical Society provides "Just Accepted" as a free service to the research community to expedite the dissemination of scientific material as soon as possible after acceptance. "Just Accepted" manuscripts appear in full in PDF format accompanied by an HTML abstract. "Just Accepted" manuscripts have been fully peer reviewed, but should not be considered the official version of record. They are accessible to all readers and citable by the Digital Object Identifier (DOI®). "Just Accepted" is an optional service offered to authors. Therefore, the "Just Accepted" Web site may not include all articles that will be published in the journal. After a manuscript is technically edited and formatted, it will be removed from the "Just Accepted" Web site and published as an ASAP article. Note that technical editing may introduce minor changes to the manuscript text and/or graphics which could affect content, and all legal disclaimers and ethical guidelines that apply to the journal pertain. ACS cannot be held responsible for errors or consequences arising from the use of information contained in these "Just Accepted" manuscripts.

ACS Publications

Analytical Chemistry is published by the American Chemical Society. 1155 Sixteenth Street N.W., Washington, DC 20036

Published by American Chemical Society. Copyright © American Chemical Society. However, no copyright claim is made to original U.S. Government works, or works produced by employees of any Commonwealth realm Crown government in the course of their duties.

Protein Binding Bends the Gold Nanoparticle Capped DNA Sequence: Towards Novel Energy-transfer based Photoelectrochemical Protein Detection

Zheng-Yuan Ma, Yi-Fan Ruan, Fei Xu, Wei-Wei Zhao, Jing-Juan Xu and Hong-Yuan Chen**

State Key Laboratory of Analytical Chemistry for Life Science and Collaborative Innovation Center of Chemistry for Life Science, School of Chemistry and Chemical Engineering, Nanjing University, Nanjing 210023, China

* To whom correspondence should be addressed.

* E-mail: zww@nju.edu.cn

* E-mail: hychen@nju.edu.cn

Abstract: In this work, we present a novel energy-transfer (ET) based photoelectrochemical (PEC) probing of DNA-protein interactions, which associates intimately with many important intracellular processes in transcriptional regulatory networks. Specifically, Au nanoparticles (NPs) were confined onto the CdS quantum dots (QDs) functionalized PEC surface by the formation of duplex DNA, the subsequent binding of the TATA-binding protein (TBP) and the resulting distortion of the Au NPs capped DNA sequence could adjust the interparticle distance and thereby modulate the PEC performance of CdS QDs through the ET process between the CdS QDs and Au NPs. Using the duplex DNA sequence as a rigid spacer, the relationship between the photocurrent quenching effect and the spacing distance was also studied and some experimental conditions were optimized, on the basis of which an novel ET-based PEC TBP biosensor was realized with high sensitivity and selectivity.

Key words：*photoelectrochemical*，*quantum dots*，*energy transfer*，*DNA binding protein,*

All the functions of DNA rely on its interactions with various proteins, and considerable proteins can specifically or nonspecifically bind to DNA for the fulfillment of their biological functions. Especially, DNA-protein interactions represent a family of intracellular processes that are fundamental in transcriptional regulatory networks including transcription, replication, recombination and repair, and such interactions have attracted increasing attentions in many disciplines.[1] In the bioanalytical field, analysts have been interested with using various techniques, e.g. traditional electrophoretic, surface enhanced resonance Raman scattering,[2] colorimetric,[3] electrochemical[4] and electrochemiluminescence (ECL),[5,6] for probing the affinity binding of proteins to DNA or their catalytic activities. For example, telomerase activity analysis through its elongation function for corresponding primer sequence was realized via a signal-on dual-potential ECL approach,[7] and the specific detections of proteins that bind to single-stranded DNA (ssDNA) and double-stranded DNA (dsDNA) were also accomplished based on the reagentless, electrochemical platform.[8] Using the photoelectrochemical (PEC) technique, we previously also demonstrated the exquisite probing of DNA-protein interaction and the TATA-binding protein (TBP) could be detected based on the steric hindrance effect easily.[9]

The PEC bioanalysis represents a newly emerged methodology that offers an elegant route for sensitive biological assays.[10-24] Despite of a rapid expansion of PEC detection formats in recent years, the essential signaling mechanisms are still quite limited due to its short development time. For instance, steric hindrance effect,[25] biocatalytic precipitation[26] and the in-situ production of electron donor/acceptor by enzyme catalysis[27] have been frequently utilized in reported works. In these strategies, recognition events were generally associated with the biological reaction to impact the solution species or the interfacial electron transfer. Because most of these formats were confined to the direct interfacial mass communication between the photoactivated sensing surface and ambient environment, the exploitation of new PEC biosensing mechanisms will be of great significance.

Energy transfer (ET) between the quantum dots (QDs) and noble metal nanoparticles (NPs) has been demonstrated as a unique phenomenon in the nanosensor field.[28] And numerous efforts have been devoted to the utilization of such ET process in various sensor systems.[29,30] In the PEC system, our

group has also demonstrated the existence of similar interplay between photoactivated QDs and Au NPs (or Ag NPs), and exploited it as an analytical basis for PEC DNA assay.[21,31] Specifically, based on the local electric fields generated from plasmon resonance of the Au NPs in close proximity, exciton states in photoactivated CdS QDs were modulated through ET effect from the CdS QDs to the Au NPs, leading to the photocurrent quenching. Due to its attractive potential, this work then catalyzed many subsequent PEC studies addressing different analytes such as heavy metal ions,[32,33] carcinoembryonic antigen,[34] thrombin,[35] etc. However, due to the short development time, the exploitation in the ET based PEC assay is still in its infancy. On the other side, recent years have witnessed the considerable developments on nanostructure designing and constructions of functional nanomaterials for numerous applications.[36-38] With specific biomolecules, QDs and NPs could offer unique platforms for engineering various biomolecule–nanomaterial hybrid systems with innovative signal-transduction mechanisms toward biomolecular detections. So, of particular interest here is to develop ingenious QDs/NPs/biomolecule nanosystem that integrated with the ET process for the advanced bioanalysis of the DNA-binding protein.

Herein, we report a novel strategy for ET based PEC detection of DNA-binding protein. Specifically, as shown in Scheme 1, through the complementary pairing between ssDNA, Au NPs was brought into the intimate distance of the CdS QDs modified on indium tin oxide (ITO) electrode for the interparticle interaction. Upon illumination, the subsequent capture of TBP by the dsDNA will further strengthen the interparticle ET via its impact on the dsDNA configuration. Specifically, the binding of the TBP would bend the Au NPs capped dsDNA, thereby placing the Au NPs closer to the CdS QDs on the electrode. With changed interparticle distance, the interparticle ET efficiency would be influenced, and the quenching effect of Au NPs on the CdS QDs could be strengthened accordingly. Besides, with dsDNA sequence as a rigid spacer, the relationship between the photocurrent intensity and the spacing distance was also studied by varying the length of dsDNA. Under optimal condition, interaction of TBP and the dsDNA probe was traced through the quenched photocurrent intensity and the TBP could be detected to the limit of 0.05 pg/mL. This work presents a novel mechanism for ET based PEC protein assay and to

the best of our knowledge has never been reported. The detailed preparation, characterization, optimization, and performance characteristics of the proposed PEC protein assay are described in the following section.

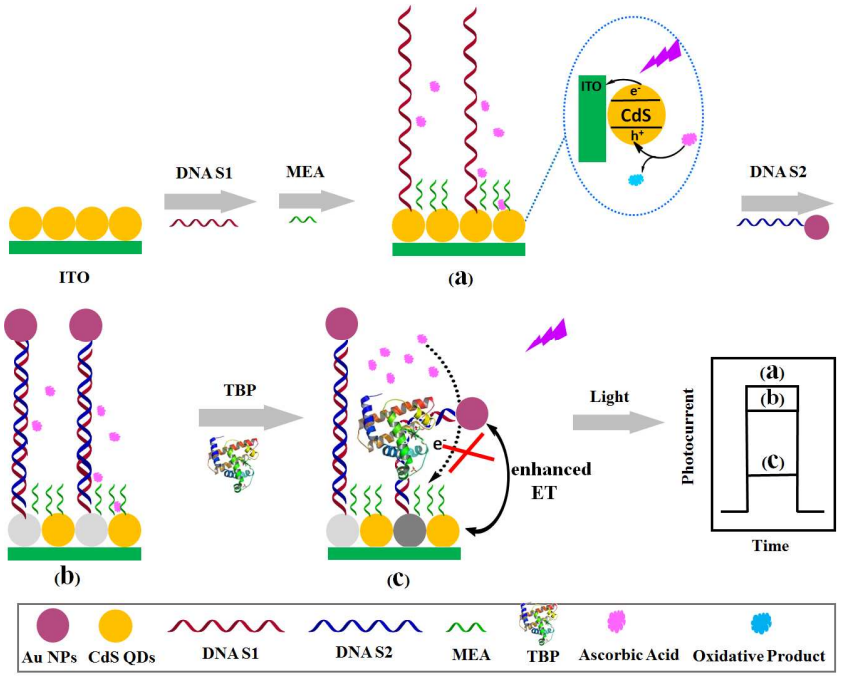

Scheme1. Schematics of the Process to Fabricate the ET-based PEC Biosensor for TBP Detection.

EXPERIMENTAL SECTION

Reagents. The ITO slices (type N-STN-S1-10, China Southern Glass Holding Co., Ltd) were used as the working electrode. 6-Mercapto-1-hexanol (MCH), tris(hydroxymethyl) aminomethane (Tris), tris(2-carboxyethyl) phosphinehydrochloride (TCEP), Poly(diallyldimethylammonium chloride) (PDDA; 20%, w/w in water, MW=200000-350000), ascorbic acid (AA), thioglycolic acid (TGA), TATA binding protein (Constituents: 20% Glycerol, 20 mM Tris HCl, 100 mM Potassium chloride, 1 mM DTT, 0.2 mM EDTA, pH 8.0), thrombin, alpha-fetoprotein (AFP), carcinoembryonic antigen (CEA) and $NaBH_4$ were obtained from Sigma Aldrich. $CdCl_2 \cdot 2.5H_2O$ was obtained from Shanghai Jinshan Tingxin Chemical Plant. $Na_2S \cdot 9H_2O$ and $HAuCl_4$ were obtained from Shanghai Lingfeng Chemical Reagent Co., LTD (Shanghai, China). Phosphate buffer solution (PBS, pH 7.4) is prepared from $Na_2HPO_4 \cdot 12H_2O$ and NaH_2PO_4. A stock solution of the DNA probe was prepared at a concentration of 100 μM in 10 mM

Tris-HCl buffer solution (pH 7.4) and was stored frozen. A solution of 10 mM Tris-HCl (pH 7.4) was used to dilute the stock solution when needed. All the other chemicals were of analytical grade. All aqueous solutions were prepared with ultrapure water (Milli-Q, Millipore).

DNA Oligonucleotides were acquired from Sangon Biotechnology Company, Ltd. (Shanghai, China) (12 bp-DNA S1，18 bp-DNA S1，24 bp-DNA S1，30 bp-DNA S1，36 bp-DNA S1，and 40 bp-DNA S1 were completely complementary with 12 bp-DNA S2，18 bp-DNA S2，24 bp-DNA S2，30 bp-DNA S2，36 bp-DNA S2，and 40 bp-DNA S2, respectively.) Except for the sequences that specifically mentioned, 30 bp-DNA was used in this work for assay application. the sequences of these oligonucleotides employed are given below and the Italic bold nucleotides were the corresponding TBP recognition section：

12 bp-DNA S1: 5'-NH_2 -AGGA***CTTTTATA***-3'

12 bp-DNA S2: 5'-SH-***TATAAAAG***TCCT-3'.

18 bp-DNA S1: 5'-NH_2-AGGA***CTTTTATA***GTGGAG-3'

18 bp-DNA S2: 5'-SH-CTCCA***CTATAAAA***GTCCT-3'.

24 bp-DNA S1: 5'-NH_2-AGGA***CTTTTATA***GTGGAGGCCGCG-3'

24 bp-DNA S2: 5'-SH-CGCGGCCTCCAC***TATAAAAG***TCCT-3'

30 bp-DNA S1: 5'-NH_2 -CCCAGGA***CTTTTATA***GTGGAGGCCGCG-3'

30 bp-DNA S2: 5'-SH-GGGCGCGGCCTCCAC***TATAAAAG***TCCTGGG-3'.

36 bp-DNA S1: 5'-NH_2 -GGGCCCAGGA***CTTTTATA***GTGGAGGCCGCGCCCGGG-3'

36 bp-DNA S2: 5'-SH-CCCGGGCGCGGCCTCCAC***TATAAAAG***TCCTGGGCCC-3'.

42 bp-DNA S1: 5'-NH_2 -CCCGGGCCCAGGA***CTTTTATA***GTGGAGGCCGCGCCCGGGCCC-3'

42 bp-DNA S2: 5'-SH-GGGCCCGGGCGCGGCCTCCAC***TATAAAAG***TCCTGGGCCCGGG-3'.

Apparatus. Transmission electron microscopy (TEM) was conducted using a JEM-2100 microscope (JEOL, Japan). Photoluminescence (PL) was measured using an RF-5301PC fluorescence spectrometer

(Shimadzu Co., Japan) equipped with a xenon lamp. UV−vis absorption spectra were obtained using a UV-3600 UV−vis−near-infrared spectrophotometer (Shimadzu, Japan). Dynamic light scattering (DLS) measurements were performed by BI-200 SM light scattering apparatus (Brookhaven Instruments Co., USA) equipped with a digital correlator at 640 nm. PEC measurements were performed with a homemade PEC system: a 5 W LED lamp with monochromatic emitting at 410 nm was used as irradiation source to produce the monochromatic illuminating light on the front of the electrode. The working electrodes were modified ITO glasses with uniform geometrical circular areas of 0.5 cm diameter, and the photocurrent signal was recorded according to our previous work.[9]

Preparation of Au NPs-Labeled DNA and SiO_2-Labeled DNA. Au NPs with average diameter 5 ± 1 nm were prepared through the reduction of $HAuCl_4$ by sodium $NaBH_4$ according to the reported methods with slight modifications. Briefly, 0.6 mL of 0.1 M ice cold $NaBH_4$ was added to 20 mL of aqueous solution containing 2.5×10^{-4} M $HAuCl_4$ under stirring, and the solution immediately turned to an orange-red color, indicating the formation of Au NPs. Then the solution was kept under stirring in the ice bath for 10 min and for another 3 h at room temperature with the color changing from orange-red to wine red. The nearly monodispersed Au NPs had an average diameter of 5 ± 1 nm as characterized by TEM and thus the final concentration of the Au colloid solution was estimated to be 6×10^{-8} M. The prepared Au NPs were kept in a refrigerator at 4 ºC for further use.

For the preparation of Au NPs-labelled DNA, 50 μL of 10μM HS-modified DNA S2 and 10 μL of 10 mM TCEP were mixed and incubated for 1 h at 37 ºC in order to reduce disulfide bonds. Then 1 mL of Au NPs (PH=7.0) was added into the above solution, and which was incubated for 16 h at room temperature under gentle shaking and dark environment. Within the above incubation step, 300 μL of 0.5 M NaCl was smoothly added into the Au-DNA solution. The resultant solution was centrifuged for 10 min at 15000 rpm and 4 ºC with 20 kD millipore. After removal of the supernatant, the precipitate was resuspended in 10 mM PBS of pH 7.4 containing 0.1 M NaCl to obtain the 1 μM Au NPs-ssDNA solution. For control experiment, the SiO_2-labelled DNA was also prepared as our previous reports.[10]

Immobilization of Au-capped DNA probe and TBP detection. The CdS QDs modified electrodes were prepared primarily according to our previous work.[9] Immobilization of DNA probe to the CdS QDs modified electrodes was accomplished via the commonly used EDC coupling reactions between COOH groups on the surface of CdS QDs and the NH_2 groups of capture DNA. The CdS QDs modified electrodes were immersed in a solution containing 10 mM EDC and 20 mM NHS for 60 min at room temperature. After rinsing, 25 μL of 1μM DNA S1 was dropped onto the surface of the electrode and incubated at 4 ºC overnight, then immersed in MEA solution (1 mM in 10 mM PBS) at the same pH for about 60 minutes to remove the nonspecifically attached DNA and simultaneously to eliminate the steric hindrance among attached DNA molecules. The surface densities of the DNA S1 modified electrode were estimated about 1.61×10^{12} strands/cm^2 according to the previous work.[9] After removal of MEA by thoroughly rinsed with 10 mM PBS solution, 25 μL of 1μM Au NPs-ssDNA was dropped onto the surface of the electrode and incubated at 37 ºC for 90 minutes to form the DNA duplex. Then the electrode was rinsed with 10 mM PBS buffer (pH 7.4) to wash off the excess Au NPs-ssDNA. The obtained QDs-duplex DNA-Au assembly was served as the work electrode in the following PEC analysis and the initial photocurrent signal is measured in 0.1 M PBS solution containing 0.1 M AA. Next, 25 μL of TBP with different concentrations were dropped onto the electrodes for an incubation of 60 minutes in moist environment at 37 ºC. Thereafter, the electrodes were rinsed with 10 mM PBS, pH 7.4, and then introduced for the respective PEC measurements.

RESULTS AND DISCUSSION

Characterization of CdS QDs and Au NPs. The morphology and sizes of the particles were determined by DSL spectrum and TEM measurement: As shown in Figure 1, the mean hydrodynamic diameters of CdS QDs and Au NPs was 5.0 ± 1 and 4.6 ± 1 nm, respectively. In the TEM image, both of the CdS QDs and Au NPs appear as quasi-spherical particles with an average size of 5.2 nm and 4.8 nm, which was identical with the DLS results. To characterize the optical properties of CdS QDs, the

photoluminescence (PL) spectrum and typical UV-vis absorption of the CdS QDs were also obtained. As shown, the absorption spectrum implies that the CdS QDs have a broad absorption range which is suitable for PEC applications. Meanwhile, a symmetrical PL emission peak centered at ca. 530 nm was observed under illumination at 410 nm, demonstrating its excellent photophysical property, which is an important factor for the following ET process. Significantly, compared to the pure Au NPs, the absorption spectrum of the Au labeled-DNA probe exhibited a maximum peak at 528 nm and the slight red shift was attributed to the change of the Au NPs surface charges caused by the oligonucleotides (Figure 1D). Apparently, the PL emission of the CdS QDs overlapped with the surface plasmon resonance (SPR) absorption of the Au NPs, which is essential for the subsequent interparticle interaction in the proposed system.

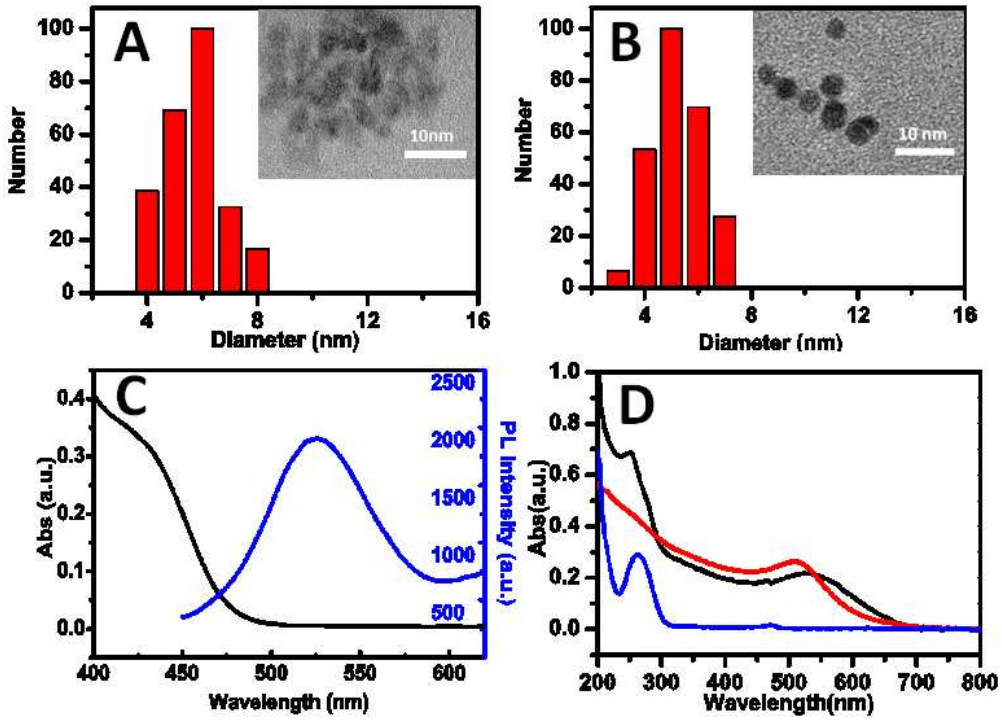

Figure 1. Hydrodynamic size distribution measured by DLS of the (A) CdS QDs and (B) Au NPs. (C) The PL spectrum (blue) and UV-vis absorption spectrum (black) of the CdS QDs, excitation wavelength: 410 nm. (D) UV-vis absorption spectrum of the Au NPs (red), ssDNA sequence (blue), and Au-labelled DNA (black). Inset of Figure A and B are the TEM images of CdS QDs and Au NPs, respectively.

Development Process of the Proposed PEC Protein Biosensor.

Interparticle distance is crucial for the excitonic response of the QDs in ET-based systems.[30,31] First,

Au NPs labelled dsDNA sequences of 12, 18, 24, 30, 36, and 42 bp were utilized as rigid spacers to modulate the interparticle spacing from 4 to 16 nm respectively (according to the assumption that 3 bp equal to 1 nm). As shown in Figure 2A, different probe length could lead to different extent of photocurrent attenuation, and the extent reduced gradually with the growth of the DNA length and it reached the bottom from 42.3% of 12 bp to 13.8% of 30 bp. From 36 bp to 42 bp, the elevation of the damping effect was then recorded. These results indicated the distance-controlled excitonic responses of CdS QDs in the ET-based PEC system, and 10 nm of interparticle distance here could cause the most remarkable signal damping, the explanation of this phenomenon will be discussed later. In our previous studies on exciton-plasmon interactions between CdS QDs and Ag NPs, such distance-dependent properties were also observed.[21] In present case, the weak quenching effect in 10 nm of 30 bp was adopted for following assay application.

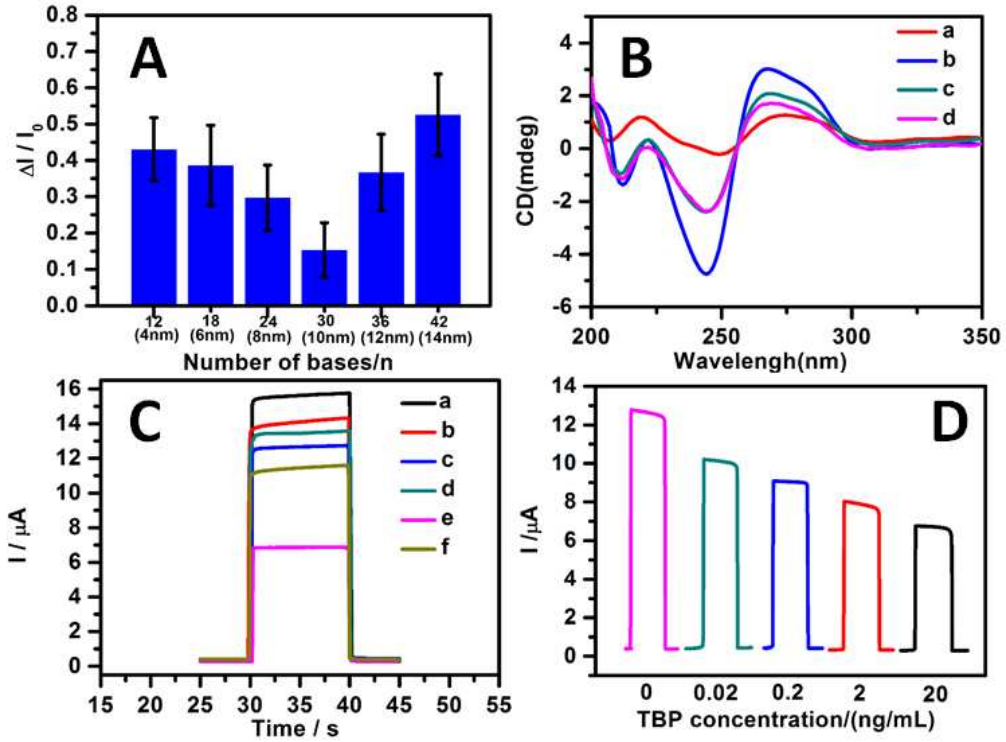

Figure 2. (A) Variation ratio of photocurrent caused by distance between CdS QDs and Au NPs from 4 nm to 14 nm. When the length of oligonucleotide sequence (concentration was 1.0×10^{-6} M) was changed, the other conditions were fixed. $\Delta I = I_0 - I$, I_0 and I are the photocurrents of ssDNA/CdS QDs/ITO electrode prior to and after hybridization, respectively. (B) CD spectra of 10 μM DNAS1 (a), 10 μM dsDNA (b), and mixture of b + 1 μM TBP (c), and 4μM TBP (d) in pH 5.3 PBS. (C) Photocurrent intensity in 0.10 M PBS containing 0.1 M AA of (a) CdS QDs/ITO electrode modified with 25 μL, 1 μM 30 bp-DNA S1 and blocked by MEA, and after hybridization with (b) bare 30 bp-DNA S2, (c) Au NPs-labelled 30 bp-DNA S2, (d) SiO_2 NPs-labelled 30 bp-DNA S2 and (e) after incubation with 20 nM TBP based on Au NPs-labelled dsDNA probe and (f) SiO_2 NPs-labelled dsDNA probe. (D) Photocurrent response of the

modified electrode after TBP incubation (0, 0.02, 0.2 20, 20 ng/mL), the DNA probe used were 30 base pairs. The PEC tests were performed in a 0.10 M PBS solution containing 0.10 M AA with 0.0 V applied voltage and 410 nm excitation light.

To test the feasibility, as shown in Figure 2B, CD spectra of ssDNA, dsDNA and DNA-protein complex were firstly recorded. Compared to the curve a of ssDNA, the dsDNA exhibited two typical CD bands of the right-handed B-helix at 248 and 274 nm, curve b. Upon addition of the target TBP, the characteristic band of dsDNA at 274 nm was reduced in magnitude, indicating the unfolding of dsDNA and the formation of DNA-protein complex, curve c. What's more, since the TBP binds to the dsDNA in a sequence-specific manner through inserting amino acid side-chains between base pairs and partially unwinding the helix,[36] as demonstrated by curve d, more TBP binding would lead to more obvious signal reduction corresponding to affected DNA secondary structure in the CD spectra.

As shown in Figure 2C, the development process of the proposed system was then monitored by the stepwise transient photocurrent responses upon the intermittent light irradiation. Curve a shows the photoresponse of the ssDNA-modified electrode. As shown in curve b and c, compared with that of bare complementary ssDNA, the photocurrent intensity exhibited a more obvious decrease after hybridized with the Au NPs-labelled ones. In a control experiment, as shown in curve d, SiO_2 NPs (ca. diameter corresponding to 5 nm) were used in place of Au NPs, and the photocurrent displayed a weaker reduction. It indicated that, upon the use of 30 bp-DNA, the interparticle ET effect was not overwhelming, while the steric hindrance also affected. After the addition of 20 ng/mL TBP, the protein would bend the dsDNA sequence at an 80 degree angle,[39] and the photocurrent decreased remarkably, curve e. In contrast, as shown in curve f, the SiO_2 NPs-labelled one displayed a much weaker signal reduction, implying that the main reason for such reduction in the Au NPs labelled system should be attributed to ET rather than steric hindrance. With the increase of TBP concentration, as shown in Figure 2D, the photocurrent responses declined gradually, indicating the feasibility of the proposed strategy.

The Discussion on the ET based PEC Process. As shown in Scheme 2, an integrated process for

the PEC response can be devided into 6 parts taking the anodic photocurrent as an example. Specifically, upon exogenous light stimulation (process1), occupied electrons in the valence band (VB) will transfer into the conduction band (CB) yielding electron–hole pairs inside the QDs (process 2). Furthermore, with valence-band holes neutralized by concomitant scavenging from the soluble donor (process 3), apart from direct electron transfer from the QDs to the electrode surface (process 4), the electron-hole pairs would also be destined for its recombination through the balance between radiative (process 5) and nonradiative (process 6) decay. As shown in process 7, when considerable spectral overlap is satisfied between the radiative emission of the CdS QDs and absorption of Au NPs, SPR of the proximal Au NPs will be excited and create local electric fields that could in turn accelerate the CdS QDs emission (process 8). Besides, along with the radiative decay, nonradiative decay rate due to energy dissipation can be also enhanced by adjacent Au NPs through the effect of exciton energy transfer (EET) (process 9).

It is worth nothing that although competition generally exists between SPR and EET in PL and ECL, it becomes a cooperative relationship in the PEC system for their overall effect contending with the electron transfer. In the present PEC system, since the concern here is the overall effect of EET and SPR on accelerating the electron-hole recombination, which relies more on the internal band gap transition as well as the PL emission,[11] some common rules could be used for the discussion about the mechanism. Exactly, most studies suggested that under certain circumstances, the final perceptible PL intensity can be depicted based on the competing factors of EET quenching and SPR enhancement as follows:

$$P_Q = \frac{1}{1+\left(\frac{R_Q}{d}\right)^{n_Q}} \quad (1)$$

$$P_E = \left(\frac{R_E}{d}\right)^{n_E} + 1 \quad (2)$$

where P_Q and P_E are the quenching factor from EET and enhancement factor from SPR, respectively; d is the QDs-metal NPs separation distance; R_Q is the Förster like radius at which 50% of the fluorescence is quenched; n_Q is a distance dependence power; R_E is a distance at which P_E becomes 2; n_E is the distance dependence power.[40] In many PL works, experimental data showed consistent results with the

theoretical derivation. Effective quenching effect can be observed while the EET process dominates within the intimate contact region for QDs-metal NPs interaction and it will turn out PL enhancement while QDs positioned in the SPR-ascendant field of the metal NPs.[41,42] For the PEC conversion process, the signals were obtained electrochemically, thus either domination between the factor of P_Q and P_E will contribute to photocurrent attenuation. What's more, since the observed photocurrent is generally the balance of several factors, it will not always change monotonically. When some integrated balance was realized between these factors at a certain distance, the photocurrent quenching would exhibit a minimum, which would explain the weakest damping effect at 10 nm in the present case.

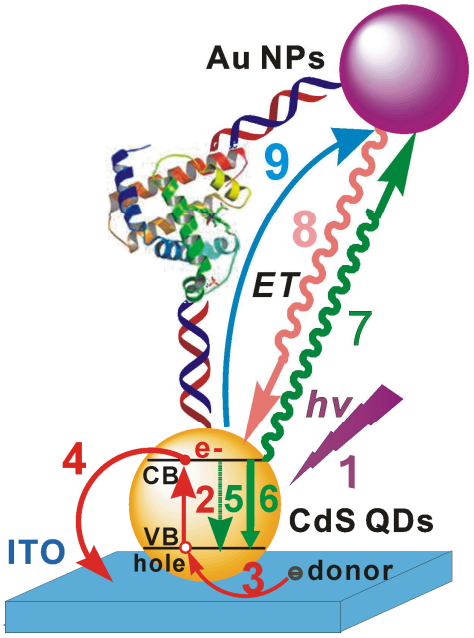

Scheme 2. Schematic mechanism of the operating PEC system. Process 1, photoexcitation of the CdS QDs; 2, photon absorption and electron transfer from the valence band (VB) to the conduction band (CB); 3, hole neutralization by electron donor; 4, electron ejection to the electrode for photocurrent generation; 5, non-radiative electron-hole recombination ; 6, radiative electron-hole recombination; 7, spontaneous emission originating from radiative decay ; 8, plasmon resonance enhancement on the radiative decay; 9, exciton energy transfer (EET) from CdS QDs to Au NPs.

Conditions Optimization. To achieve better analytical performance, several experimental parameters such as Au NP labelled-ssDNA (Au-ssDNA) concentration, the hybridization time of the target protein, the irradiation wavelength and the length of dsDNA probe were optimized. As shown in Figure 3A, the photocurrent was diminished with the Au-ssDNA concentration up to 1.0 μM and exhibited no further decrease with extra addition of the Au-ssDNA. In consequence, 1.0 μM of Au-

ssDNA was employed for the following use. The impact of irradiation wavelength on the photocurrent response was also studied under different wavelength light stimulation. Owing to the limitations of weak light emission from the Xe lamp in short wavelength region and slight absorbance of CdS QDs under long wavelength, the effective irradiation scope was set within the range of 300 nm to 550 nm. As shown in Figure 3B, the photocurrent response of the CdS QDs showed an obvious quenching effect within the range of 350 nm to 450 nm, and 410 nm was used as excitation wavelength for following uses. With increasing incubation time, as shown in Figure 3C, the photocurrent attenuation was enhanced and then reached a plateau after 60 minutes, suggesting the DNA-protein interaction was completely finished. Thus, 60 minutes was selected as the final incubation time. In presence of 20 ng/mL TBP, the extent of PEC reduction was further investigated with the probe length variation. As shown in Figure 3D, in agreement with previous studies, 30 bp could invoke a more noticeable quenching effect.

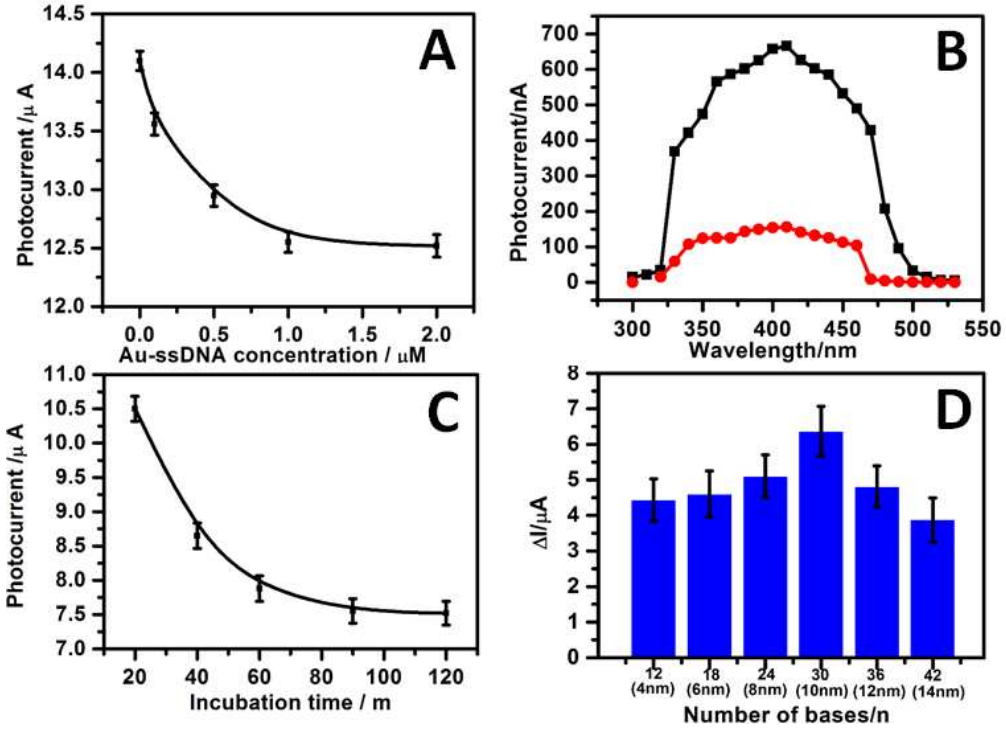

Figure 3. Effects of (A) Au NPs labelled-ssDNA concentration, (B) irradiation wavelength, (C) incubation time for TBP and (D) dsDNA probe length on the photocurrent response of the biosensor. For photocurrent record before (dark) and after (red) ET quenching, the change of irradiation wavelength was realized using a 500 W Xe lamp equipped with monochromator as irradiation source. The PEC tests were performed in a 0.10 M PBS solution containing 0.10 M AA with 0.0 V applied voltage and dsDNA probe of 30 bases under 410 nm excitation. When dsDNA probe length or excitation wavelength were changed, the other conditions were fixed.

Analytical Performances. Since the degree of signal reduction is directly related to the target

concentration, the PEC TBP bioassay could be accomplished via tracking the photocurrent variation. Figure 4A displays the resulted photocurrents after incubation with TPB of variable concentrations and the inset figure shows the corresponding derived calibration curve. As shown, the photocurrent decrement was proportional to the TBP concentrations in a linear range from 0.1 pg/mL to 20 ng/mL, suggesting the TBP controlled distortion of the dsDNA and thus the quenching effect. After 20 ng/mL, the growth trend of the signal attenuation began to flatten, indicating the near saturation of the DNA-protein binding. The detection limit was experimentally found to be 0.05 pg/mL, which exhibited a noticeable improvement compared with our earlier work based on the steric hindrance effect.[9] In addition, we further compared this proposed PEC protocol with other reported works addressing TBP detection.[43-47] As listed in Table 1, this ET-based PEC biosensor possessed excellent analytical performance among these TBP biosensors.

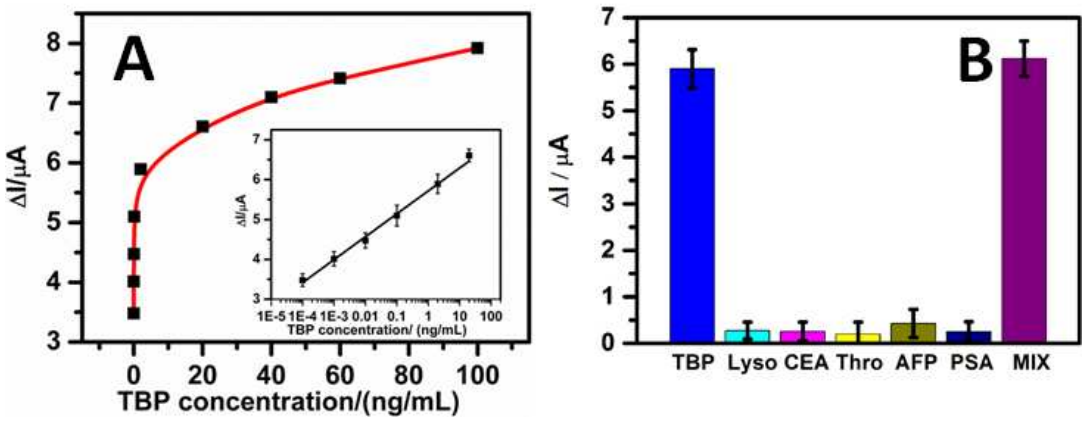

Figure 4. (A) Effect of different TBP concentrations on the photocurrent responses. $\Delta I = I-I_0$, I_0 stands for the photocurrent of the modified electrode before TBP capturing and I was the final photocurrent after incubation with TBP of elevated concentrations from 0.1 pg/mL to 100 ng/mL respectively. The inset is the corresponding derived calibration curve. Error bars represent the standard deviation of triplicates. (B) Effects of other proteins on the detection of 10 ng/mL TBP in 0.1 M PBS (pH 7.0) at the bias voltage of 0 V and following the visible light irradiation (λ=410 nm). The bars represent 200 ng/mL Lysozyme, CEA, Thro, AFP, PSA and a mixture of six kinds of proteins, respectively. Error bars represent the standard deviation of three replicates.

The selectivity of the proposed biosensor was also evaluated. The as-fabricated biosensor was incubated in sample solutions containing different interfering agents such as alpha-fetoprotein (AFP), carcinoembryonic antigen (CEA), lysozyme (Lyso), prostate specific antigen (PSA), and thrombin (Thro), as well as the mixed solution of these six kinds of proteins under the same experimental

conditions. As shown in Figure 4B, the results demonstrated that none of these proteins exhibited obvious signal decrease except the target protein and the mixed sample, implying the good selectivity of the biosensor that could be attributed to the high affinity of the TBP towards the TATA box. The reproducibility of this biosensor was further assessed through an interassay relative standard deviation (RSD). By assaying five 10 ng/mL TBP samples under the same conditions, satisfactory reproducibility was confirmed with the RSD of 8.52%. The stability of the protein biosensor was also examined by performing the detection of 10 ng/mL TBP. After 10 times repeated measurements, the photocurrent was unchanged over time, indicating the stable readout for signal collection. Furthermore, after 15 days of storage in PBS buffer (pH 7.4) at 4 ºC, this PEC biosensor retained 92.5% of the original intensity. Besides, since TBP binds specifically to the dsDNA through inserting amino acid side-chains between base pairs and partially unwinding the helix, we currently could not separate the protein from the dsDNA for repeated use.

Table 1. Analytical Performance of Various TBP biosensors

analyte	measurement protocol	linear range	detection limit	reference
TBP	electrochemical bioassay	40 pM to 25.4 nM	10.6 pM	25
TBP	electrochemical bioassay	4 nM to 12 nM	2 nM	4
TBP	electrochemical impedance spectroscopy	0.8 nM to 68.8 nM	0.8 nM	27
TBP	microelectrodes based electrochemical bioassay	3 nM to 300 nM	3 nM	26
TBP	surface enhanced resonance raman scattering	1 nM to 80 nM	-	2
TBP	fluorescent beacon	10 nM to 1000 nM	5.8 nM	28
TBP	fluorescent-amplified strategy	100 fM to 1 nM	40.7 fM	29
TBP	electrochemiluminescence detection	0.2 nM to 100 nM	0.02 nM	5
TBP	amplified electrochemiluminescence detection	0.015 nM to 150 nM	5 pM	6
TBP	colorimetric bioassay	0 to 120 nM	10 nM	3
TBP	label-free PEC bioassay	0.4 ng/mL to 400 ng/mL (0.01 nM to 10.26 nM)	0.04 ng/mL (1 pM)	9
TBP	ET-based PEC bioassay	0.1 pg/mL to 20 ng/mL (2.6 fM to 512.8 pM)	0.05 pg/mL (1.28 fM)	this work

CONCLUSIONS

This work has successfully fabricated a novel ET based PEC biosensor for sensitive probing of DNA-protein interactions through modulating the PEC performance of CdS QDs by Au NPs. In our model system, the binding of the TBP onto the Au NPs capped dsDNA would bend the dsDNA configuration, rendering the Au NPs more closer to the CdS QDs on the electrode and thereby influencing the interparticle ET efficiency. With the varied quenching effect of Au NPs on CdS QDs, the changed photocurrent intensity could be signalled for the elegent tracking of the protein binding. Besides, the in-depth investigation on the relationship between the Au NPs-CdS QDs interparticle distance and the corresponding ET effect in the PEC system was also conducted for the first time. Upon bioinduced variation of interparticle ET effect, this work provided a feasible protocol for PEC TBP detection with high sensitivity and selectivity. More significantly, integrated with proper biological systems, this strategy could serve as a general basis for probing other biorecognition events or biocatalytic transformations.

ASSOCIATED CONTENT

AUTHOR INFORMATION

Corresponding Authors

* E-mail: zww@nju.edu.cn

* E-mail: hychen@nju.edu.cn

Notes

The authors declare no competing financial interest.

ACKNOWLEDGMENT

Financial support from the 973 Program (Grant 2012CB932600), the National Natural Science Foundation of China (Grant Nos.21327902, 21135003 and 21305063), the Natural Science Funds of

Jiangsu Province (Grant BK20130553). This work was also supported by a Project Funded by the Priority Academic Program Development of Jiangsu Higher Education Institutions.

REFERENCES

(1) Ren, B.; Robert, F.; Wyrick, J. J.; Aparicio, O.; Jennings, E. G.; Simon, I.; Zeitlinger, J.; Schreiber, J.; Hannett, N.; Kanin, E.; Volkert, T. L.; Wilson, C. J.; Bell, S. P.; Young, R. A. *Science* **2000**, *290*, 2306.

(2) Bonham, A. J.; Braun, G.; Pavel, I.; Moskovits, M.; Reich, N. O. *J. Am. Chem. Soc.* **2007**, *129*, 14572.

(3) Ou, L. J.; Jin, P. Y.; Chu, X.; Jiang, J. H.; Yu, R. Q. *Anal. Chem.* **2010**, *82*, 6015.

(4) Ricci, F.; Bonham, A. J.; Mason, A. C.; Reich, N. O.; Plaxco, K. W. *Anal. Chem.* **2009**, *81*, 1608.

(5) Wang, J.; Zhao, W. W.; Zhou, H.; Xu, J. J.; Chen, H. Y. *Biosens. Bioelectron.* **2013**, *41*, 615.

(6) Wang, J.; Zhao, W. W.; Li, X. R.; Xu, J. J.; Chen, H. Y. *Chem. Commun.* **2012**, *48*, 6429.

(7) Zhang, H. R.; Wu, M. S.; Xu, J. J.; Chen, H. Y. *Anal. Chem.* **2014**, *86*, 3834.

(8) Zhao, P.; Zhou, L. F.; Nie, Z.; Xu, X. H.; Li, W.; Huang, Y.; He, K. Y.; Yao, S. Z. *Anal. Chem.* **2013**, *85*, 6279.

(9) Ma, Z. Y.; Ruan, Y. F.; Zhang, N.; Zhao, W. W.; Xu, J. J.; Chen, H. Y. *Chem. Commun.* **2015**, *51*, 8381.

(10) Zhao, W. W.; Xu, J. J.; Chen, H. Y. *Chem. Soc. Rev.* **2015**, *44*, 729.

(11) Zhao, W. W.; Wang, J.; Zhu, Y. C.; Xu, J. J.; Chen, H. Y. *Anal. Chem.* **2015**, *87*, 9520.

(12) Zhao, W. W.; Xu, J. J.; Chen, H. Y. *Chem. Rev.* **2014**, *114*, 7421.

(13) Tang, J.; Zhang, Y. Y.; Kong, B.; Wang, Y. C.; Da, P. M.; Li, J.; Elzatahry, A. A.; Zhao, D. Y.; Gong, X. G.; Zheng, G. F. *Nano Lett.* **2014**, *14*, 2702.

(14) Zayats, M.; Kharitonov, A. B.; Pogorelova, S. P.; Lioubashevski, O.; Katz, E.; Willner, I. *J. Am. Chem. Soc.* **2003**, *125*, 16006.

(15) Haddour, N.; Chauvin, J.; Gondran, C.; Cosnier, S. *J. Am. Chem. Soc.* **2006**, *128*, 9693.

(16) Wang, L. N.; Ma, W. G.; Gan, S. Y.; Han, D. X.; Zhang, Q. X.; Niu, L. *Anal. Chem.* **2014**, *86*, 10171.

(17) Zhuang, J. Y.; Lai, W. Q.; Xu, M. D.; Zhou, Q.; Tang, D. P. *ACS Appl. Mater. Interfaces* **2015**, *7*, 8330.

(18) Chen, D.; Zhang, H.; Li, X.; Li, J. H. *Anal. Chem.* **2010**, *82*, 2253.

(19) Li, H. N.; Mu, Y. W.; Yan, J. R.; Cui, D. M.; Ou, W. J.; Wan, Y. K.; Liu, S. Q. *Anal. Chem.* **2015**, *87*, 2007.

(20) Long, Y. T.; Kong, C.; Li, D. W.; Li, Y.; Chowdhury, S.; Tian, H. *Small* **2011**, *12* , 1624.

(21) Zhao, W. W.; Yu, P. P.; Shan, Y.; Wang, J.; Xu, J. J.; Chen, H. Y. *Anal. Chem.* **2012**, *84*, 5892.

(22) Wang, J.; Liu, Z. H.; Hu, C. G.; Hu, S. S. *Anal. Chem.* **2015**, *87*, 9368.

(23) Li, Z.; Xin, Y.; Zhang, Z. *Anal. Chem.* **2015**, *87*, 10491.

(24) Zhang, X. R.; Guo, Y. S.; Liu, M. S.; Zhang, S. S. *RSC Adv.* **2013**, *3*, 2846.

(25) Kang, Q.; Yang, L. X.; Chen, Y. F.; Luo, S. L.; Wen, L. F.; Cai, Q. Y.; Yao, S. Z. *Anal. Chem.* **2010**, *82*, 9749.

(26) Zhao, W. W.; Ma, Z. Y.; Yu, P. P.; Dong, X. Y.; Xu, J. J.; Chen, H. Y. *Anal. Chem.* **2012**, *84*, 917.

(27) An, Y. R.; Tang, L. L.; Jiang, X. L.; Chen, H.; Yang, M. C.; Jin, L. T.; Zhang, S. P.; Wang, C. G.; Zhang, W. *Chem.-Eur. J.* **2010**, *16*, 14439.

(28) Kulakovich, O.; Strekal, N.; Yaroshevich, A.; Maskevich, S.; Gaponenko, S.; Nabiev, I.; Woggon, U.; Artemyev, M. *Nano Lett.* **2002**, *2*, 1449.

(29) Shimron, S.; Cecconello, A.; Lu, C. H.; Willner, I. *Nano Lett.* **2013**, *13*, 3791.

(30) Wang, J.; Shan, Y,; Zhao, W. W.; Xu, J. J.; Chen, H. Y. *Anal. Chem.* **2011**, *83*, 4004.

(31) Zhao, W. W.; Tian, C. Y.; Xu, J. J.; Chen, H. Y. *Chem. Commun.* **2012**, *48*, 895.

(32) Zang, Y.; Lei, J. P.; Hao, Q.; Ju, H. X. *ACS Appl. Mater. Interfaces* **2014**, *6*, 15991.

(33) Zhao, M.; Fan, G. C.; Chen, J. J.; Shi, J. J.; Zhu, J. J. *Anal. Chem.* **2015**, *87*, 12340.

(34) Zeng, X. X.; Ma, S. S.; Bao, J. C.; Tu, W. W.; Dai, Z. H. *Anal. Chem.* **2013**, *85*, 11720.

(35) Fan, G. C.; Zhu, H.; Shen, Q.; Han, L.; Zhao, M.; Zhang, J. R.; Zhu, J. J. *Chem. Commun.* **2015**, *51*, 7023.

(36) Ariga, K.; Yamauchi, Y.; Rydzek, G.; Ji, Q.; Yonamine, Y.; Wu, K. C. W.; Hill, J. P. *Chem. Lett.* **2014**, *43*, 36.

(37) Wegst, U. G. K.; Bai, H.; Saiz, E.; Tomsia, A. P.; Ritchie, R. O. *Nat. Mater.* **2015**, *14*, 23.

(38) Pieters, B. J. G. E. van Eldijk, M. B.； Nolte, R. J. M.； Mecinović, J. *Chem. Soc. Rev.* **2016**, *45*, 24.

(39) Delgadillo, R. F.; Whittington, J. E.; Parkhurst, L. K.; Parkhurst, L. J. *Biochemistry* **2009**, *48*, 1801.

(40) Kim, D.; Yokota, H.; Taniguchi, T.; Nakayama, M. *J. Appl. Phys.* **2013**, *114*, 154307.

(41) Song, M.; Wu, B. T.; Chen, G. X.; Liu, Y.; Ci, X. T.; Wu, E.; Zeng, H. P. *J. Phys. Chem. C* **2014**, *118*, 8514.

(42) Ribeiro, T.; Prazeres, T. J. V.; Moffitt, M.; Farinha, J. P. S. *J. Phys. Chem. C* **2013**, *117*, 3122.

(43) Zhang, Y.; Liu, F.; Nie, J. F.; Jiang, F. Y.; Zhou, C. B.; Yang, J. N.; Fan, J. L.; Li, J. P. *Analyst* **2014**, *139*, 2193.

(44) Gorodetsky, A. A.; Ebrahim, A.; Barton, J. K. *J. Am. Chem. Soc.* **2008**, *130*, 2924.

(45) Chang, H. X.; Li, J. H. *Electrochem. Commun.* **2009**, *11*, 2101.

(46) Vallée-Bélisle, A.; Bonham, A. J.; Reich, N. O.; Ricci, F.; Plaxco, K. W. *J. Am. Chem. Soc.* **2011**, *133*, 13836.

(47) Li, C. X.; Qiu, X. Y.; Hou, Z. H.; Deng, K. Q. *Biosens. Bioelectron.* **2015**, *64*, 505.

for TOC only